Polyketides Hot Paper

How to cite:
International Edition: doi.org/10.1002/anie.202110658
German Edition: doi.org/10.1002/ange.202110658

Biochemistry-Guided Prediction of the Absolute Configuration of Fungal Reduced Polyketides

Junya Takino, Akari Kotani, Taro Ozaki, Wenquan Peng, Jie Yu, Yian Guo, Susumu Mochizuki, Kazuya Akimitsu, Masaru Hashimoto, Tao Ye, Atsushi Minami,* and Hideaki Oikawa**

Abstract: *Highly reducing polyketide synthases (HR-PKSs) produce structurally diverse polyketides (PKs). The PK diversity is constructed by a variety of factors, including the β-keto processing, chain length, methylation pattern, and relative and absolute configurations of the substituents. We examined the stereochemical course of the PK processing for the synthesis of polyhydroxy PKs such as phialotides, phomenoic acid, and ACR-toxin. Heterologous expression of a HR-PKS gene, a trans-acting enoylreductase gene, and a truncated non-ribosomal peptide synthetase gene resulted in the formation of a linear PK with multiple stereogenic centers. The absolute configurations of the stereogenic centers were determined by chemical degradation followed by comparison of the degradation products with synthetic standards. A stereochemical rule was proposed to explain the absolute configurations of other reduced PKs and highlights an error in the absolute configurations of a reported structure. The present work demonstrates that focused functional analysis of functionally related HR-PKSs leads to a better understanding of the stereochemical course.*

Introduction

Fungal highly reducing polyketide synthases (HR-PKSs) are multifunctional enzymes for synthesis of the backbone structure of biologically active polyketides (PKs), including cholesterol-lowering lovastatin, virulence factor T-toxin, and the squalene synthase inhibitors zaragozic acids. HR-PKSs have a single set of catalytic domains whose organization resembles with that of fatty acid synthases (FASs).[1–4] Although both HR-PKSs and FASs use the catalytic domains repeatedly in their chain elongation processes, they differ in the programming of their β-keto processing domains. In the case of HR-PKSs, the β-keto processing domains operate to varying extents during iteration, thereby affording structurally diverse PKs.[1,2] The structural diversity can also be attributed to a variety of other factors, including the chain length and methylation pattern. In bacterial PKSs, the absolute configurations of the stereogenic centers are predicted by motif analysis and the programming rule. However, a similar corresponding rule has not been established for fungal HR-PKSs.

During PK processing, HR-PKSs generate acyl carrier protein (ACP)-tethered intermediates with multiple stereogenic centers. Understanding the stereochemical course leading to fungal PKs is important in the functional analysis of HR-PKSs. Direct prediction of the stereochemical course from the structure of natural PKs is difficult because: 1) The hydroxy group installed by a ketoreductase (KR) domain is frequently lost during PK processing. As a result, in many cases fungal PKSs give simple polyenes or saturated fatty acids with few substituents. 2) Post-PKS oxidation installs additional oxygen functionalities, making it difficult to determine the origin of the oxygen atom without experimental support. 3) In some cases, a single KR domain produces the products having hydroxy groups with different configurations,[5,6] preventing understanding of the stereochemical rule for HR-PKS catalysis. To overcome these problems, administration of isotopically labeled precursors and in vitro enzymatic reactions using a recombinant protein have provided insight into the stereospecificity of the individual HR-PKS.[7,8] However, to our knowledge, unified understanding of the stereochemical course of the HR-PKS synthesis of structurally and biosynthetically related fungal PKs is limited because of the lack of focused analysis of functionally related HR-PKSs, which hampers the proposal of a general mechanism for HR-PKSs.

The most reliable method to elucidate the stereospecificity of HR-PKSs is in vitro analysis.[8] However, this method requires protein expression optimization and purification. Recently, heterologous expression of HR-PKSs in fungal versatile hosts has become a practical method for functional analysis.[9] This is an effective alternative to in vitro analysis

[*] J. Takino, A. Kotani, Dr. T. Ozaki, Dr. A. Minami, Prof. Dr. H. Oikawa
Department of Chemistry, Faculty of Science, Hokkaido University
Sapporo 060-0810 (Japan)
E-mail: aminami@sci.hokudai.ac.jp
hoik@sci.hokudai.ac.jp
W. Peng, Dr. J. Yu, Dr. Y. Guo, Prof. Dr. T. Ye
State Key Laboratory of Chemical Oncogenomics, Peking University Shenzhen Graduate School
Xili, Nanshan District, Shenzhen 518055 (China)
E-mail: yet@pkusz.edu.cn
Dr. S. Mochizuki, Prof. Dr. K. Akimitsu
International Institute of Rare Sugar Research and Education & Faculty of Agriculture, Kagawa University
Kagawa, 761-0795 (Japan)
Prof. Dr. M. Hashimoto
Faculty of Agriculture and Life Science, Hirosaki University
Hirosaki 036-8561 (Japan)
Dr. J. Yu, Dr. Y. Guo
School of Biotechnology and Health Sciences, Wuyi University
Jiangmen 529020 (China)
Supporting information and the ORCID identification number(s) for the author(s) of this article can be found under: https://doi.org/10.1002/anie.202110658.

These are not the final page numbers!

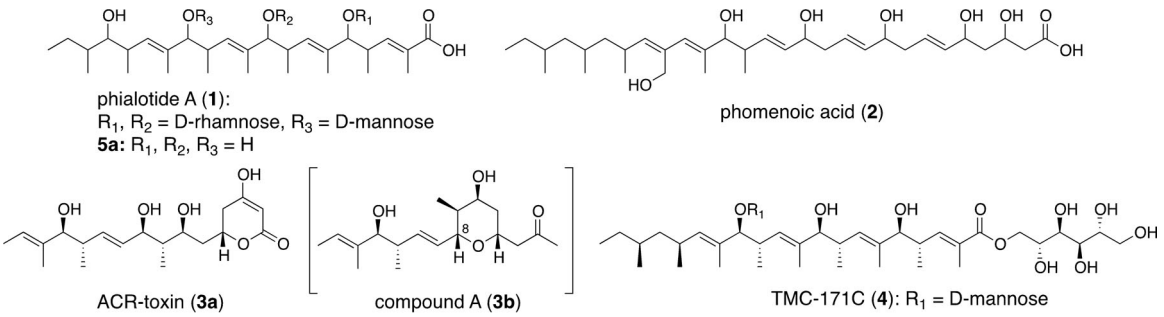

Figure 1. Chemical structures of fungal polyhydroxy polyketides.

because of the high versatility of PKS expression. Based on the background described above, we hypothesized that a small group of functionally related HR-PKSs share the same stereochemical course, and therefore the focused analysis of such HR-PKSs may provide a general mechanism of PKS processing.

In this article, we describe the functional analysis of HR-PKSs that produce polyhydroxy PKs with multiple stereogenic centers, such as phialotide A (**1**),[10] phomenoic acid (PMA, **2**),[11] and ACR-toxin (**3a**)[12] (Figure 1). Determination of the relative and absolute configurations of an unmodified PK by degradation studies enabled us to propose a general stereochemical rule for the PK processing. This rule was successfully applied to related PKS families that produce different polyhydroxy PKs; however, violations of the rule were found for several reported configurations in thermolides. This prompted us to examine computational chemical shift predictions and synthetic studies of the model compound, resulting in the proposal of a revised structure. We also discuss the extensive application of the rule to other HR-PKSs.

Results and Discussion

Recently, a putative biosynthetic gene cluster (BGC), *phom*, that is involved in the biosynthesis of **2** was identified by gene silencing experiments and quantitative reverse transcriptase PCR analysis.[13] The HR-PKS gene, *phomA* (previous name: PKS2), accompanies four genes: a trans-ER (t-ER) gene (*phomB*), a cytochrome P450 gene (*phomE*), a functionally unknown gene (*phomD*), and a transcription factor. Considering the structural similarity between **1** and **2** that possess multiple numbers of substituents, including a hydroxy group, an *E*-olefin, and a branched methyl group, which are regularly installed on the single PK chain to form an alternately repeating a dehydrated and a non-dehydrated substructure (Figure 1), we hypothesized that a HR-PKS gene as well as modification genes are highly conserved in the BGC of **1**. A BLAST search allowed us to identify a putative BGC (*phia*) in the genome of *Pseudophialophora* sp. BF-0158, which produces **1** (Figure S1 and Table S1). The BGC includes the four homologous genes described above: HR-PKS (PhiaA); 58% (identity), t-ER (PhiaB); 63%, unknown protein (PhiaD); 42%, and cytochrome P450 (PhiaE); 33%. An NRPS gene, *phiaC*, was also identified in *phia* BGC. The homologous NRPS (PhomC, 39% identity) was found near the proposed BGC of **2**. Although the expression profile of the NRPS gene was different from that of PKS2,[13] the NRPS gene is conserved in other homologous BGCs found in *Stagonospora nodorum* and *Metharhizium acridum*.[13] Taken together, we hypothesized that PhiaA-E are candidates participating in the biosynthesis of **1**.

To determine whether the identified genes are sufficient for production of the PK chain of **1**, we constructed transformants, AO-*phiaABCD*, AO-*phiaABC*, AO-*phiaAB*, and AO-*phiaAC*. The AO-*phiaABCD* produced new product **5a** ($C_{29}H_{50}O_6$), which was named as prophialotide (Figure 2). The ^1H and ^{13}C NMR data of **5a** resembled those of the PK part of **1**. Extensive 2D NMR analysis revealed a planar structure.

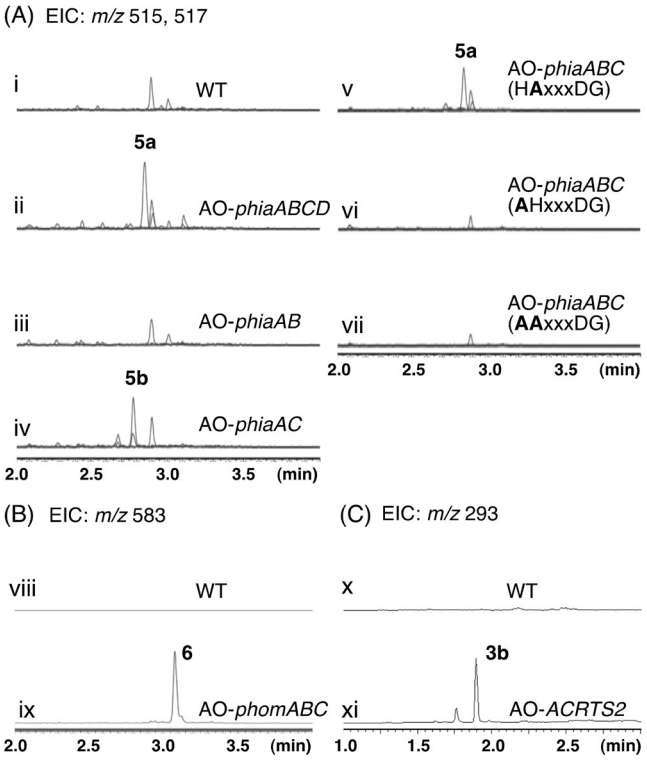

Figure 2. UPLC-MS profiles of the metabolites from transformants harboring biosynthetic genes of A) phialotide, B) phomenoic acid, and C) ACR-toxin. i) AO-*WT*, ii) AO-*phiaABC*, iii) AO-*phiaAB*, iv) AO-*phiaAC*, v) AO-*phiaABC*(HAxxDG mut.), vi) AO-*phiaABC*(AHxxDG mut.), vii) AO-*phiaABC*(AAxxDG mut.), viii) AO-WT, ix) AO-*phomABC*, *x*) AO-*WT*, and xi) AO-*ACRTS2*.

MS/MS analysis showed fragmentation ion peaks that reflected the repeated substructure (Figure S2). **5a** has all the oxygen and methyl substituents found in **1**, suggesting they are installed by the collaborative action of PhiaA and PhiaB. To determine the relative and absolute configurations, we prepared two alcohols, **7-1** and **8-1** (single isomer), by ozonolysis of **5a** followed by a reductive workup with $NaBH_4$ (Figures 3 and S3). In the case of **7-1**, we synthesized four diastereomers as synthetic standards (STDs) from known compounds (Scheme S1). Chiral GC/MS analysis showed that the relative configuration of **7-1** was determined to be (2*S*,3*R*,4*S*) by comparison with the STDs **7-1a**–**7-1d**. This was further supported by ^{1}H NMR analysis (Figure S3). The relative configuration of **8-1** was determined in a similar manner using synthetic STDs **8-1a** (*anti*) and **8-1b** (*syn*) (Scheme S1). The retention time of the benzylidene acetal **8-2** was the same as that of **8-2a**. The absolute configurations of the degradation products were then determined after the derivatization to both (*R*)-MαNP and (*S*)-MαNP esters.[14] UPLC-MS analysis showed that **7-2** and **8-3** were identical to **7-2a** and **8-3a**, respectively. We therefore concluded that the absolute configuration of **5a** was (4*S*,5*S*,8*S*,9*S*,12*S*,13*S*,16*S*,17*R*,18*S*).

UPLC-MS analysis of the metabolites from other transformants showed that AO-*phiaABC* produced **5a** while AO-*phiaAB* did not, suggesting that the hypothetical protein PhiaD is not essential for the production of **5a**, but a truncated NRPS, PhiaC, is indispensable. AO-*phiaAC*, which lacks a trans-ER gene (*phiaB*) produced a new metabolite **5b** ($C_{29}H_{48}O_6$) (Figure 2). 1D and 2D NMR analyses revealed that this is a non-reduced product of **5a**, possessing an *E*-olefin at the methyl-terminal position (Scheme 1). MS/MS analysis supported this proposed structure.

We then turned our attention to the hydrolysis of the ACP-tethered intermediate because PhiaA has no chain-releasing domain such as a thioesterase (TE) domain. Given the fact that **5a** was produced only in the transformants harboring *phiaC*, we hypothesized that PhiaC, a truncated NRPS lacking a thiolation (T) domain, mediates the hydrolysis reaction instead of a canonical condensation reaction. The proposed hydrolysis was examined by mutational analysis, with particular focus on the active site HHxxxDG motif of the C domain[15] because the C domain catalyzes reactions such as intramolecular lactonization (C–O bond formation) and amide bond formation using an amino acid.[15] Three mutants (H**A**xxxDG, **A**HxxxDG, and A**A**xxxDG) were constructed and co-expressed with PhiaA and PhiaB in *A. oryzae*. The transformant possessing an H**A**xxxDG mutant produced **5a**, while the other transformants did not, strongly suggesting that the C domain mediates the hydrolysis reaction (Figure 2).

Identification of three essential enzymes for **5a** production enabled us to examine the heterologous production of the PK chain of **2**. We prepared two plasmids, pDP801:*phomA* and pDP201:*phomBC*, and introduced them into *A. oryzae* to construct AO-*phomABC*. UPLC-MS analysis of the metabolites from AO-*phomABC* showed the production of new metabolite **6** ($C_{34}H_{58}O_7$), of which molecular formula is identical to that of deoxy derivative of **2** lactone isolated from the producer (Figure 2 and Scheme 1).[11] The structure was confirmed by 1D and 2D NMR analysis. Similar to the process used for the analysis of **5a**, we conducted an ozonolysis of **6** to obtain four fragments, **8-1**, **9-1**, **10-1** (single isomer), and **11-1**, to determine their absolute configurations (Figures 3 and S3). The absolute configuration of **8-1** was determined to be (2*S*,3*S*). Similar to the procedures used for **8-1**, we applied a stepwise derivatization of **10-1** and determined the absolute configuration as 2*S*. For **9-1**, we synthesized four chiral STDs, **9-1a**–**9-1d**, and the racemic mixture **9-1e**. Chiral GC-MS analysis showed that **9-1** had the same retention time as **9-1a**, which had a (2*S*,4*S*,6*S*) configuration. UPLC-MS analysis of the (*S*)-MαNP derivative further supported the absolute configuration of **9-1**. In the case of **11-1**, we synthesized two diastereomers, **11-1a** and **11-1b**. They were derivatized with (*S*)-MαNP acid to afford **11-2a** and **11-2b**, which were separable by UPLC-MS with a non-chiral column. The chromatographic behavior of **11-2** was the same as **11-2a**, but different from the corresponding (*R*)-MαNP derivative **11-3a**, demonstrating that **11-1** had an (3*R*,5*S*) configuration. Taken together, the absolute configuration of **6** was determined to be (3*R*,5*S*,9*S*,13*S*,16*S*,17*S*,22*S*,24*S*,26*S*).

To obtain further insight into the stereochemical course of this type of PK, we then conducted a heterologous expression of the ACRTS2 involved in the biosynthesis of **3a** because ACRTS2 exhibits homology with PhiaA (55% identity) and PhomA (68%). Because t-ER is not essential for synthesis of the PK backbone of **3a**, we introduced an ACRTS2 gene into *A. oryzae* to construct AO-*ACRTS2*. Metabolite analysis showed the production of **3b** ($C_{18}H_{30}O_4$) as a major product (Figure 2 and Scheme 1), which is known as a decarboxylation product of ACR-toxin.[12] The NMR data and optical rotation value ($[\alpha]_D^{22} = +58$ [lit. $[\alpha]_D^{21} = +44$]) were in good agreement with those previously reported. The proposed decarboxylation mechanism to afford **3b** is shown in Scheme S2. Currently, we speculate that an intramolecular non-enzymatic cyclization affords **3a** as in the case of shimalactone biosynthesis.[16]

Based on the above results, we were able to propose the PK processing leading to **5**, **6**, and **3a** (Schemes 1 and S3). The biosynthetic Scheme to synthesize **5a** and **5b** is summarized in Scheme 1. The characteristic repeating substructure is constructed by successive dehydration (DH) skipping and enoyl reduction (ER) skipping during PK processing. During the PK processing of **5** and **6**, t-ER reduces the double bond of the α,β-unsaturated thioester in the initial stage to yield a saturated thioester. Considering that **6** has a 1,3-*syn* dimethyl structure, this methyl-terminal enoyl reduction is likely a characteristic feature of this type of PK. After processing, the ACP-tethered PK subsequently undergoes hydrolysis by a truncated NRPS to afford a linear PK. To our knowledge, a truncated NRPS that catalyzes hydrolysis is rare in fungal PK biosynthesis.

We then turned our attention to the stereochemical course used to synthesize **5**, **6**, and **3a** (Scheme 2). To simplify discussions about the stereogenic centers, we are applying a newly defined $^oR/^oS$ model that focuses on the direction of the PK chain elongation and does not consider the absolute configurations of other substituents located nearby. Following

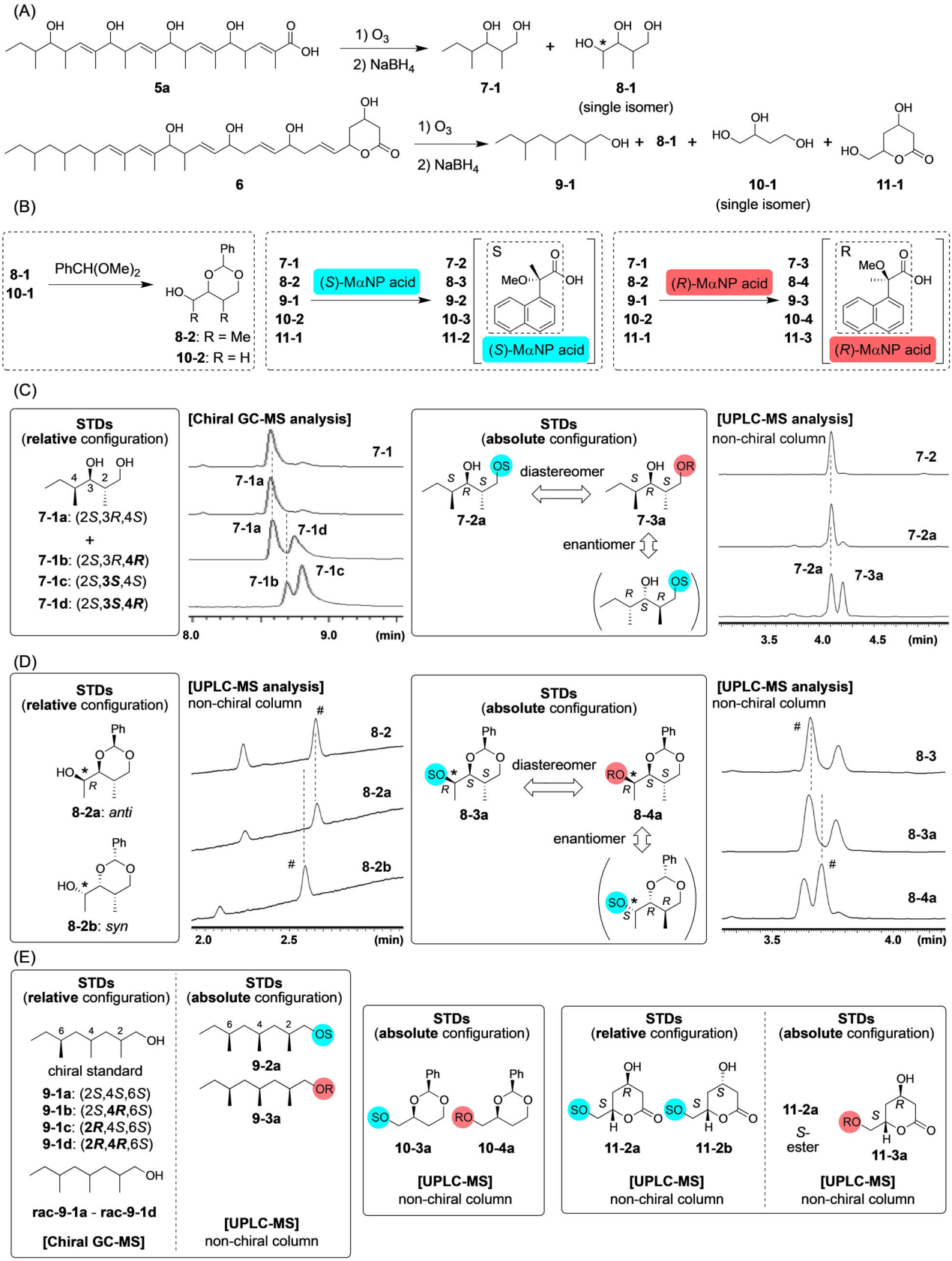

Figure 3. A) Chemical degradation of **5a** and **6**. Degradation product **8-1** was obtained as diastereomeric mixture at the C4 position labeled by an asterisk, which was installed by the $NaBH_4$ reduction of the ozonolysis product. B) Derivatization of the ozonolysis products. C) Determination of the absolute configuration of **7-1**. D) Determination of the absolute configuration of **8-1**. To simplify the discussions, we focused on the major isomers, which are labeled with #. E) Chemical structures of the synthetic standards.

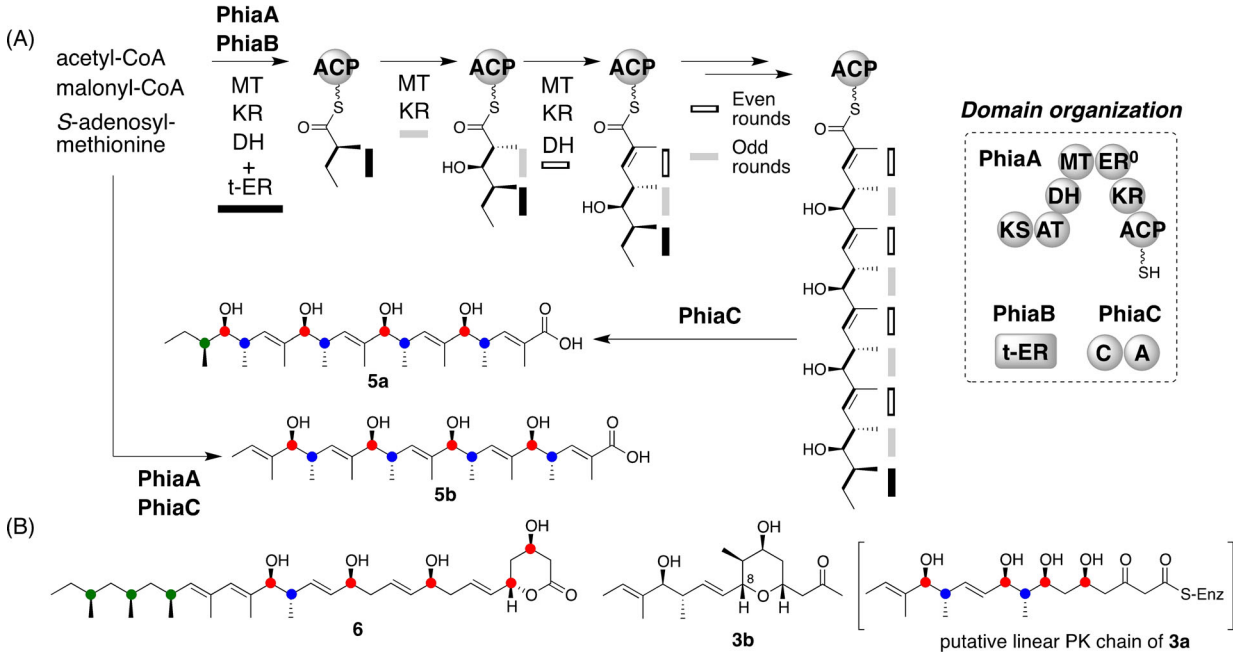

Scheme 1. A) Proposed biosynthetic pathways of **5a** and **5b**. Domain organizations of PhiaA-C are enclosed by a dotted line. B) Chemical structures of **6** and **3b** synthesized by PhomABC and ACRTS2, respectively. Their proposed biosyntheses are summarized in the Supplementary Information. Carbons with a substituent installed by MT, KR, and ER domain are labeled with blue, red, and green circle, respectively. These labels are used in the following figures and schemes.

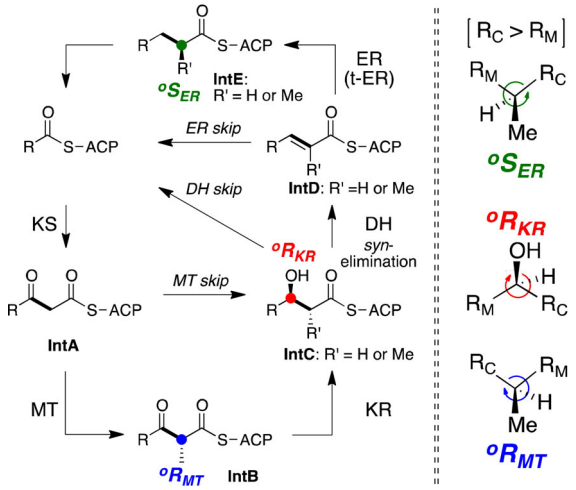

Scheme 2. Stereochemical course leading to polyketides classified into PMA, TML, and PSL groups. In our stereochemical model, we defined that a carboxy terminal chain (R_C) has higher priority than a methyl terminal chain (R_M). The configuration is described by a capital letter and the domain used to install the substituent is described by a subscript.

the formation of **IntA**, the methyltransferase (MT) domain installs an $^{o}R_{MT}$-methyl group at the α position to give **IntB**, which is reduced by the KR domain to yield **IntC** with an $^{o}R_{KR}$-hydroxy group. The hydroxythioester then undergoes *syn*-elimination to afford **IntD** with an *E*-olefin by the action of a dehydratase (DH) domain. This stereochemical course leading to an *E*-olefin via an ^{o}R-hydroxythioester indicates a close stereochemical and biosynthetic relationships between the three domains in the PK chain processing. The final enoyl reduction by t-ER gives **IntE** possessing an $^{o}S_{ER}$-methyl group. This stereochemical course is basically the same as that of fatty acid biosynthesis.[7,17]

Polyhydroxy PKs are an emerging family of fungal PKs, although they are a relatively small group (Figures 4 and S4). Polyhydroxy PKs can be divided into three groups according to the PK chain-releasing mechanism. The first PMA group consists of linear PKs with a terminal carboxylic acid such as **1** and **2** (Figure S4), which is hydrolyzed by a truncated NRPS. The second TML group is a macrolactam family PKs represented by thermolide (TML),[18] which are composed of a polyhydroxy PK and an amino acid (Figure S4). The PK construction is catalyzed by HR-PKS with an active ER domain. The characteristic macrolactam moiety is constructed by a complete NRPS composed of condensation (C), adenylation (A), thiolation (T), and terminal condensation-like (C_T) domains (Figure S5). This group includes metacridamides,[19] georatusin,[20] and valactamides.[21] The third PSL group is a macrolactone family of PKs represented by phaeospelide A (PSL)[22] (Figure S4). The characteristic macrocyclization is catalyzed by a stand-alone TE. Unlike HR-PKSs for PMA and TML PKs, HR-PKSs in the macrolactone family lack the MT domain. This domain organization is consistent with the fact that representative macrolactone PKs, such as decarestrictine C1 (HR-PKS; DcsA),[23] AKMLA (AkmlA),[24] and CIMLA (CimlA),[24] have no branched methyl group.

To obtain insight into the biosynthetic relationship of these three polyhydroxy PK groups, we conducted a phylogenetic analysis as reported in our recent studies on PKS-NRPS hybrids[25] (Figure S6). When focusing on functionally characterized HR-PKSs, we find three distinct clades correspond-

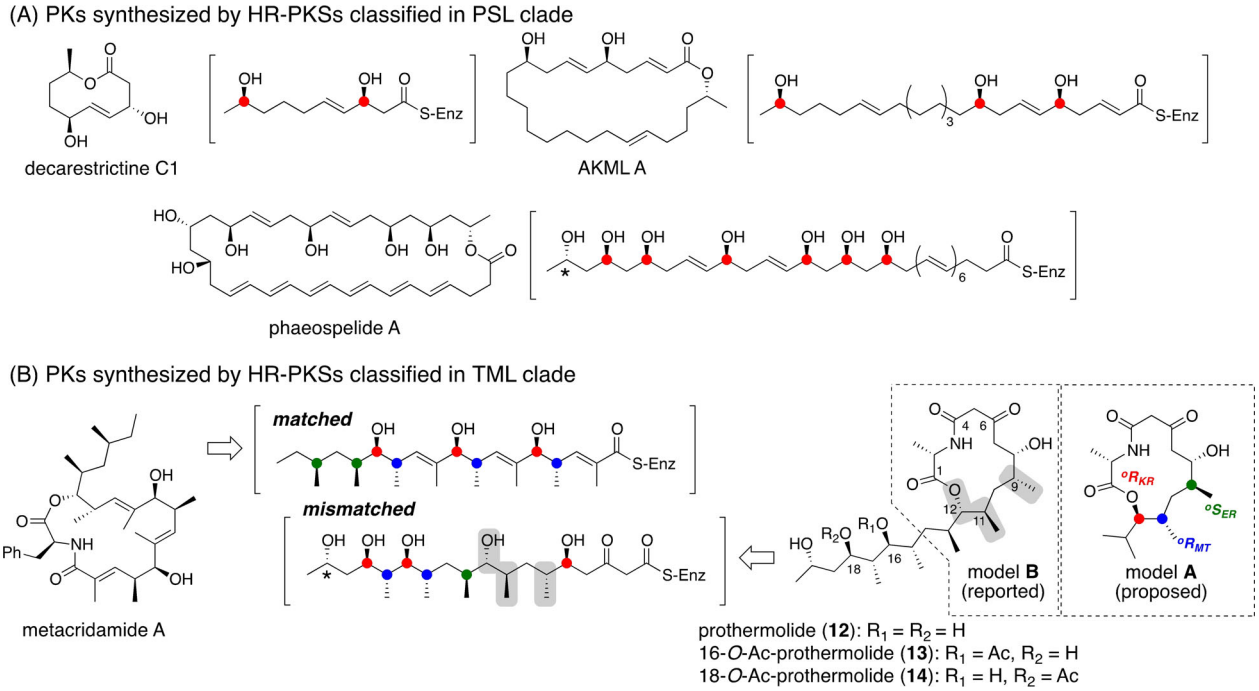

Figure 4. Chemical structures of PKs synthesized by HR-PKSs in the A) PSL clade and B) TML clade. The putative ACP-tethered intermediate is described in the brackets. A mismatched stereochemistry is labeled by an asterisk. Three sereogenic centers found in thermolide that were re-examined by ab initio NMR chemical shift calculations, are highlighted by the grey color.

ing to the PMA (linear PKs), TML (macrolactam PKs), and PSL (macrolactone PKs) groups. In the case of the former PMA and TML clades, either NRPS or the truncated NRPS catalyze the cleavage of the PK chain from HR-PKS. In contrast, in the PSL clade, a stand-alone TE catalyzes this cleavage. Taken together, we found that phylogeny-based classification of HR-PKSs is useful for predicting the type of chain-releasing mechanism, which directly reflects the structure of the PKs. Indeed, the PMA clade includes HR-PKSs from a producer of cubensic acid (strain; *Xylaria cubensis*) and TMC-171 (*Clonostachys rosea*) (Figure 1), of which the structures of the PK moiety resemble those of **1**–**3**.

The PMA group of PKs, such as **5**, **6**, and **3a**, commonly have ${}^{o}R_{MT}$, ${}^{o}R_{KR}$, and ${}^{o}S_{ER}$ configurations installed by HR-PKS/t-ER (Scheme 2). This stereochemical rule can explain the absolute configurations of the structurally related TMC-171 (**4**),[26] of which its producer, *C. rosea*, has a single BGC classified into the PMA clade (Figure 1). Presuming that the PMA clade BGCs found in *Xylaria* sp. are involved in the biosynthesis of structurally related PKs such as cubensic acid (producer: *Xylaria cubensis*),[27] malaysic acid (*Xylaria* sp.),[28] berteric acid (*Xylaria* sp.),[28] and cameronic acid (*Xylaria* sp.)[28] (Figure S1), we can predict the absolute configurations based on the proposed stereochemical course (Figure S4).

Based on the established backbone structures of macrocyclic PKs in the TML and PSL groups (Figures 4 and S4), we also propose that the stereochemical course can basically be applied to PKs such as metacridamide A (TML group). Exceptional PK is thermolides.[18] The reported absolute configuration of the macrolactam moiety of thermolides, prothermolide (pTML, **12**), 16-*O*-Ac-pTML (**13**), and 18-*O*-Ac-pTML (**14**), is (2*S*,8*S*,9*R*,11*R*,12*S*). The configurations at positions 9, 11, and 12 violate the proposed stereochemical rule. To re-examine the absolute configuration on the macrocyclic ring, we performed DFT-based NMR chemical shift calculations[29] for model compounds simplified the side chain with an isopropyl group using Hehre's protocol. DP4 probability analysis showed that, among 16 possible diastereomers, the probability for model compound **B**, which has the reported configuration (9*R*,11*S*,12*S*), was only 0.3 % when Goodman's parameters ($\sigma = 2.306$ ppm, $\nu = 11.38$) were used. The analysis also suggested an exclusively high probability for the predicted (9*S*,11*R*,12*R*) model compound **A** (87.2 %) (Figure S7).

To obtain conclusive evidence that model compound **A** represents the relative configuration of the corresponding fragment of the natural substance, an asymmetric synthesis of **A** was carried out as shown in Scheme 3. The synthesis thus commenced with the stereoselective hydrogenation of the known α,β-unsaturated imide **15**[30] over Pd/Al_2O_3 to afford **16** as a mixture of two diastereomers (4:1 by ^{1}H NMR).[31] After chromatographic purification, the major diastereomer **16** was obtained in 72 % yield. The hydroxyl group of **16** was next protected as a Bn ether with benzyl trichloroacetimidate (**17**), followed by reductive removal of the chiral auxiliary with $NaBH_4$ to provide the primary alcohol **18** in 91 % yield over two steps. Treatment of alcohol **18** with TCCA and TEMPO[32] afforded the corresponding aldehyde, which was subjected to a vinylogous aldol reaction under Krüger and Carreiras copper-catalyzed conditions[33] with silyloxy diene **19** to give rise to β-hydroxy dioxinone **20** in 65 % yield and a diastereomeric ratio (>99:1) favoring the desired *syn*

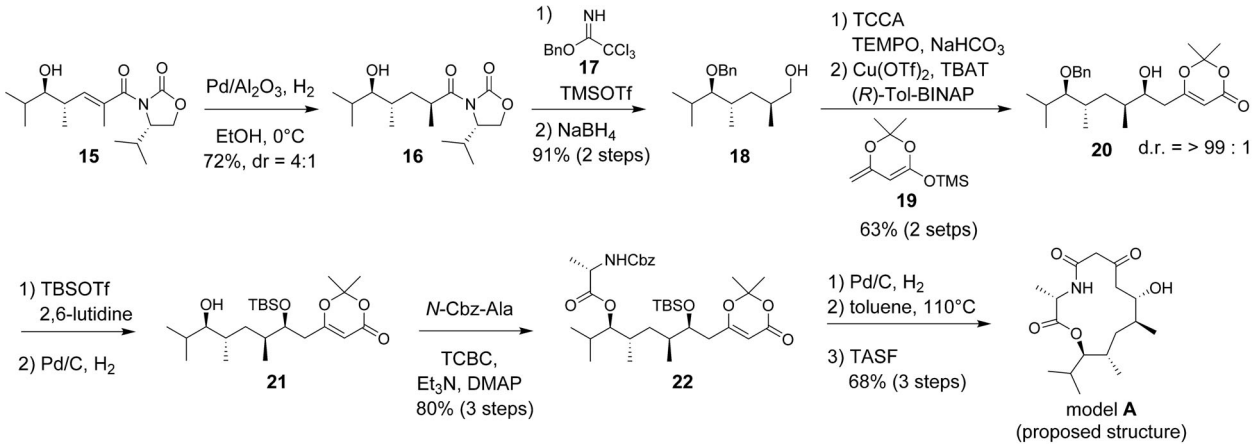

Scheme 3. Synthesis of model compound **A**. TCCA = trichloroisocyanuric acid, TBAT = tetrabutylammonium difluorotriphenylsilicate, TCBC = 2,4,6-trichlorobenzoyl chloride, TASF = tris(dimethylamino)sulfonium difluorotrimethylsilicate.

adduct. Protection of **20** as its TBS ether and hydrogenolytic removal of the benzyl ether to afford the corresponding alcohol **21**, which was then condensed with Cbz-Ala under Yamaguchi conditions, furnished **22** in 80% yield over three steps. Hydrogenolysis of the Cbz protecting group cleanly afforded the amine, which was heated in toluene at reflux under dilute conditions resulted in macrocyclization to give the expected β-ketoamide[34] followed by deprotection of the TBS ether with TASF, provided **A** in 68% yield over three steps. The ^{13}C-NMR spectrum of **A** was nearly identical to those of **12**–**14** (macrocyclic ring). The deviations of the ^{13}C NMR chemical shifts of the synthetic model compound **A** with **12**–**14** are within ± 0.7 ppm (Figure S8). Based on the results, we propose a structural revision of the absolute configurations on the macrolactam moiety of the thermolides. This is a good example that the stereochemical rule is useful for predicting the absolute configurations of known PKs that have been classified into TML and PSL clades.

Given the close relationship between the MT, KR, and DH domains, the stereospecificity of the ketoreduction is a key issue for understanding the stereochemical course catalyzed by HR-PKSs. Based on the well-established stereochemical model for bacterial PKSs that A type and B type KRs install $^{o}S_{KR}$- and $^{o}R_{KR}$-configurations, respectively,[35] we examined motif analysis of the KR domains of fungal HR-PKSs. We found that the KR domains of most HR-PKSs, including HR-PKSs in PMA, TML, and PSL clades, as well as mammalian FAS, have characteristic motifs found in bacterial B-type KRs (Figure S10). Representative HR-PKSs with a B-type_KR domain include SQTKS (natural product, squalestatin),[9b] CazF (chaetoviridin),[36] LovB and LovF (lovastatin),[37] GLPKS4 (pneumocandin),[38] and EasB (emericellamide)[39] (Figure 5), which synthesize a PK chain with $^{o}R_{KR}$-OH. These results suggest that most HR-PKSs afford an $^{o}R_{KR}$-OH during PK processing to synthesize an *E*-olefin (Figure S11). Indeed, Cox and co-workers demonstrated that the DH domain of SQTKS catalyzes a *syn*-elimination of an $^{o}R_{KR}$-hydroxythioester to give an *E*-olefin.[8] It should also be notable that functionally characterized HR-PKSs described above make distinct clades different from PMA/TML/PSL clades (Figure S6). Given the fact that HR-PKSs in PMA/TML/PLS clades synthesize a PK chain via the ^{o}R-hydroxythioester, HR-PKSs classified into those new clades may catalyze PK processing in the same stereospecific manner. In contrast to the MT, KR, and DH domains, the ER domain can act independently, as seen in the case of mFAS and bacterial multimodular PKS.[7,17] Although the $^{o}S_{ER}$ configuration is predominant (Figure S11), there are PKs possessing all $^{o}R_{ER}$ configurations, such as fumonisin B1, betaenone, and scyphostatin (Figure S12). This optional selectivity has been retained during evolution of the HR-PKSs to synthesize structurally diverse PKs.

There are a few exceptions to the proposed stereochemical rule that have mismatched stereochemistry (Figures 5, S4, and S13). For example, phaeospelide A is a PSL-type PK that possesses an $^{o}S_{KR}$-configuration at the methyl-terminal position (Figure S4). Given the fact that all of the remaining hydroxy groups have $^{o}R_{KR}$ configuration, the stereochemical violation occurs only in the first round of PK processing. A similar observation is found in resorcylic acid lactones and structurally related derivatives such as hypothemycin,[5,6,40] dehydrocurvularin,[41] and monocerin[42] (Figure S13). Stereochemical violation at a methyl-terminal position is also observed in other domains. The DH domain of Fus1 involved in fusarin biosynthesis gives a *Z*-olefin at the methyl-terminal position,[43] while the same DH domain generates an *E*-configurated polyene backbone (Figure 5). Considering that, in general, a *Z*-olefin is synthesized by *syn*-elimination of an $^{o}S_{KR}$-hydroxythioester during PK processing,[44] the methyl-terminal *Z*-olefin found in fusarin is likely constructed via an $^{o}S_{KR}$-hydroxythioester. Similar *Z*-olefin formation has also been reported in the biosynthesis of aminoacylated products.[45] In addition, t-ERs in the biosynthesis of atpenin[46] and aspyridone[47] generate an $^{o}R_{ER}$-methyl group in the first round of PK processing (Figure S13), although they generate $^{o}S_{ER}$-configurations in later steps. Detailed functional analysis of each domain would provide insight into the site-specific configurational violations found in those PKs. However, when we exclude these minor examples, the prediction rule is otherwise applicable to fungal reduced PK metabolites.

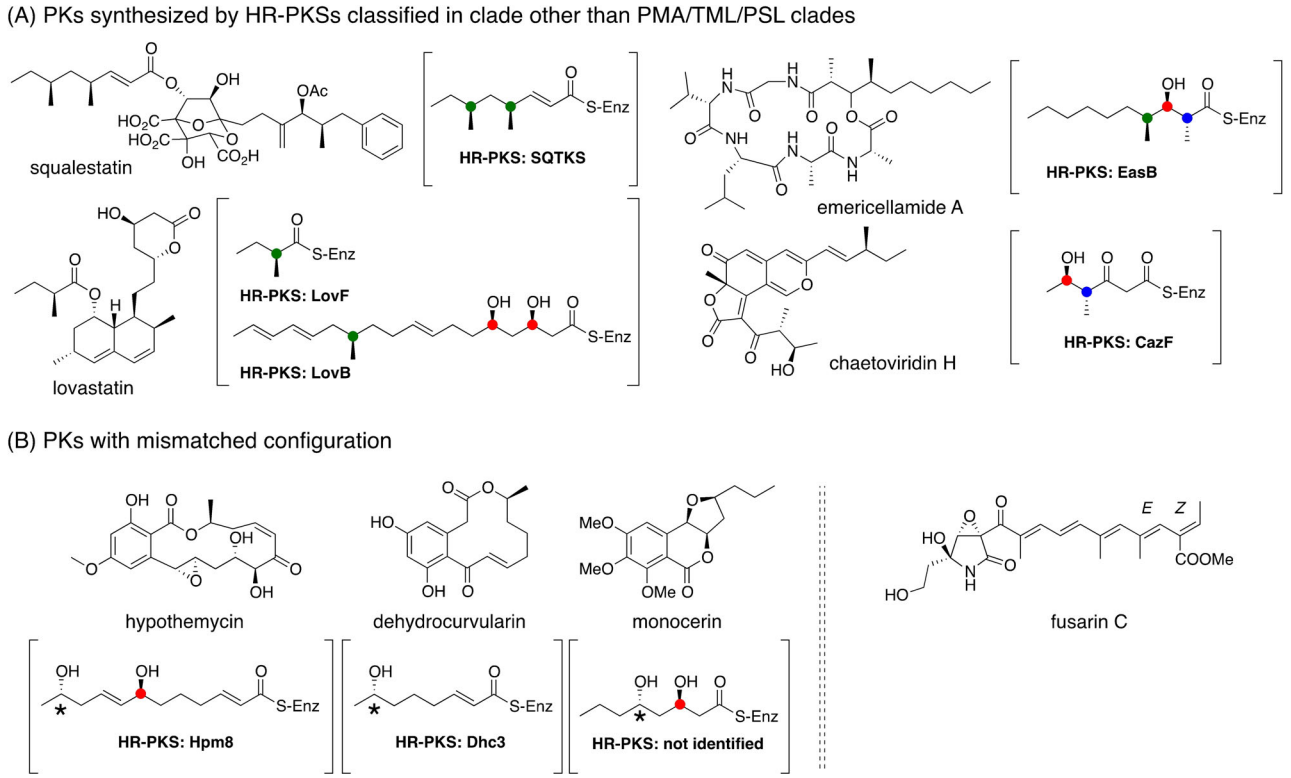

Figure 5. A) Chemical structures of PKs synthesized by HR-PKSs in other clades. B) Examples of PKs with mismatched stereochemistry. The corresponding ACP-tethered intermediate is described in the brackets.

Conclusion

In this study, we elucidated a unified stereochemical course for polyhydroxy PKs, phialotides, phomenoic acid, and ACR-toxin by determining the relative and absolute configurations of the unmodified PKs synthesized by HR-PKS. The proposed stereochemical rule explains the absolute configurations of other polyhydroxy PKs in PMA, TML, and PSL groups, and highlights errors in the reported absolute configurations on the macrolactam moiety of thermolides. Computation-assisted chemical shift prediction and a synthetic study of model compound **A**, which lacks the side chain of prothermolide, allowed us to propose a structural revision. The proposed stereochemical rule is helpful for the structural revision and prediction of fungal polyhydroxy PKs. Our present work demonstrates that focused functional analysis of functionally related HR-PKSs based on the phylogenetic analysis is effective for understanding the stereochemical course of PK processing.

Acknowledgements

We are grateful to Prof. Hiroshi Tomoda for giving us a phialotides producer, *Pseudophialophora* sp. BF-0158. This work was financially supported by Japan Society for the Promotion of Science Grants [16H06446 (A.M.), 17K19214 (A.M.), 19H02835 (A.M.), and 19H02891 (H.O.)]. The work also conducted by the U.S. Department of Energy Joint Genome Institute, a DOE Office of Science User Facility, supported under Contract No. DE-AC02-05CH11231 (H.O.). T.Y. acknowledges financial support from the Shenzhen Peacock Plan (KQTD2015071714043444).

Conflict of Interest

The authors declare no conflict of interest.

Keywords: bioinformatics analysis · fungal polyketides · heterologous expression · polyketide synthase · stereochemical course

[1] R. J. Cox, *Org. Biomol. Chem.* **2007**, *5*, 2010 – 2026.
[2] Y.-H. Chooi, Y. Tang, *J. Org. Chem.* **2012**, *77*, 9933 – 9953.
[3] D. A. Herbst, C. A. Townsend, T. Maier, *Nat. Prod. Rep.* **2018**, *35*, 1046 – 1069.
[4] J. Wang, J. Liang, L. Chen, W. Zhang, L. Kong, C. Peng, C. Su, Y. Tang, Z. Deng, Z. Wang, *Nat. Commun.* **2021**, *8*, 867.
[5] H. Zhou, Z. Gao, K. Qiao, J. Wang, J. C. Vederas, Y. Tang, *Nat. Chem. Biol.* **2012**, *8*, 331 – 333.
[6] W. Ding, Y. Li, Q. Zhang, *ACS Chem. Biol.* **2015**, *10*, 1590 – 1598.
[7] J. D. Bu'Lock, T. J. Simpson in *Biosynthesis, Vol. 6* (Eds.: J. D. Bu'Lock), Royal Society of Chemistry, London, **1980**, pp. 1 – 39.
[8] a) E. Liddle, A. Scott, L.-C. Han, D. Ivison, T. J. Simpson, C. L. Willis, R. J. Cox, *Chem. Commun.* **2017**, *53*, 1727 – 1730; b) D. M. Roberts, C. Bartel, A. Scott, D. Ivison, T. J. Simpson, R. J. Cox, *Chem. Sci.* **2017**, *8*, 1116 – 1126.
[9] a) J. Kennedy, K. Auclair, S. G. Kendrew, C. Park, J. C. Vederas, C. R. Hutchinson, *Science* **1999**, *284*, 1368 – 1372; b) R. J. Cox, F. Glod, D. Hurley, C. M. Lazarus, T. P. Nicholson, B. A. M. Rudd, T. J. Simpson, B. Wilkinson, Y. Zhang, *Chem. Commun.* **2004**,

2260 – 2261; c) S. M. Ma, J. W.-H. Choi, H. Zhou, K. K. M. Lee, V. A. Moorthie, X. Xie, J. T. Kealey, N. A. Da Silva, J. C. Vederas, Y. Tang, *Science* **2009**, *326*, 589 – 592; d) T. Ugai, A. Minami, R. Fujii, M. Tanaka, K. Gomi, H. Oikawa, *Chem. Commun.* **2015**, *51*, 1878 – 1881.

[10] A. Yagi, R. Uchida, K. Kobayashi, H. Tomoda, *J. Antibiot.* **2020**, *73*, 211 – 223.

[11] a) M. Devys, J. P. Férézou, R. S. Topgi, M. Barbier, *J. Chem. Soc. Perkin Trans. 1* **1984**, 2133 – 2137; b) M. Devys, R. S. Topgi, J.-P. Férézou, L. Quaino, J.-F. Bousquet, A. Kollmann, M. Barbier, *Phytochemistry* **1986**, *25*, 531 – 532.

[12] a) J. M. Gardner, Y. Kono, J. H. Tatum, Y. Suzuki, S. Takeuchi, *Phytochemistry* **1985**, *24*, 2861 – 2867; b) J. M. Gardner, Y. Kono, J. H. Tatum, Y. Suzuki, S. Takeuchi, *Agric. Biol. Chem.* **1985**, *49*, 1235 – 1238.

[13] C. E. Elliott, D. L. Callahan, D. Schwenk, M. Nett, D. hoffmeister, B. J. Howlett, *Fungal Genet. Biol.* **2013**, *53*, 50 – 58.

[14] In this study, we used MαNP acid instead of α-methoxy-α-(trifluoromethyl)phenylacetic acid (MTPA) as a chiral derivatizing agent because separation of the resultant diasteromers is always superior to that of the corresponding MTPA esters. a) Y. Kasai, J. Naito, S. Kuwahara, M. Watanabe, A. Ichikawa, N. Harada, *J. Synth. Org. Chem. Jpn.* **2004**, *62*, 1114 – 1127; b) N. Harada, *Molecules* **2016**, *21*, 1328.

[15] R. D. Süssmuth, A. Mainz, *Angew. Chem. Int. Ed.* **2017**, *56*, 3770 – 3821; *Angew. Chem.* **2017**, *129*, 3824 – 3878.

[16] I. Fujii, M. Hashimoto, K. Konishi, A. Unezawa, H. Sakuraba, K. Suzuki, H. Tsushima, M. Iwasaki, S. Yoshida, A. Kudo, R. Fujita, A. Hichiwa, K. Saito, T. Asano, J. Ishikawa, D. Wakana, Y. Goda, A. Watanabe, M. Watanabe, Y. Masumoto, J. Kanazawa, H. Sato, M. Uchiyama, *Angew. Chem. Int. Ed.* **2020**, *59*, 8464 – 8470; *Angew. Chem.* **2020**, *132*, 8542 – 8548.

[17] D. H. Kwan, F. Schulz, *Molecules* **2011**, *16*, 6092 – 6115.

[18] a) J.-P. Guo, C.-Y. Zhu, C.-P. Zhang, Y.-S. Chu, Y.-L. Wang, J.-X. Zhang, D.-K. Wu, K.-Q. Zhang, X.-M. Niu, *J. Am. Chem. Soc.* **2012**, *134*, 20306 – 20309; b) J.-M. Zhang, H.-H. Wang, X. Liu, C.-H. Hu, Y. Zou, *J. Am. Chem. Soc.* **2020**, *142*, 1957 – 1965.

[19] S. B. Krasnoff, U. Englich, P. G. Miller, M. L. Shuler, R. P. Glahn, B. G. G. Donzelli, D. M. Gibson, *J. Nat. Prod.* **2012**, *75*, 175 – 180.

[20] Y.-M. Shi, C. Richter, V. L. Challinor, P. Grün, A. G. del Rio, M. Kaiser, A. Schüffler, M. Piepenbring, H. Schwalbe, H. B. Bode, *Org. Lett.* **2018**, *20*, 1563 – 1567.

[21] K. D. Clevenger, J. W. Bok, R. Ye, G. P. Miley, M. H. Verdan, T. Velk, C. Chen, K. Yang, M. T. Robey, P. Gao, M. Lamprecht, P. M. Thomas, M. N. Islam, J. M. Palmer, C. C. Wu, N. P. Keller, N. L. Kelleher, *Nat. Chem. Biol.* **2017**, *13*, 895 – 901.

[22] Y. Morishita, H. Zhang, T. Taniguchi, K. Mori, T. Asai, *Org. Lett.* **2019**, *21*, 4788 – 4792.

[23] D.-W. Gao, C. S. Jamieson, G. Wang, Y. Yan, J. Zhou, K. N. Houk, Y. Tang, *J. Am. Chem. Soc.* **2021**, *143*, 80 – 84.

[24] Y. Morishita, Y. Aoki, M. Ito, D. Hagiwara, K. Torimaru, D. Morita, T. Kuroda, H. Fukano, Y. Hoshino, M. Suzuki, T. Taniguchi, K. Mori, T. Asai, *Org. Lett.* **2020**, *22*, 5876 – 5879.

[25] A. Minami, T. Ugai, T. Ozaki, H. Oikawa, *Sci. Rep.* **2020**, *10*, 13556.

[26] J. Kohno, Y. Asai, M. nishio, M. Sakurai, K. Kawano, H. hiramatsu, N. Kameda, N. Kishi, T. Okuda, S. Komatsubara, *J. Antibiot.* **1999**, *52*, 1114 – 1123.

[27] R. L. Edwards, D. J. Maitland, A. J. S. Whalley, *J. Chem. Soc. Perkin Trans. 1* **1991**, 1411 – 1417.

[28] M. O. Adeboya, R. L. Edwards, T. Laessoee, D. J. Maitland, *J. Chem. Res. Synop.* **1995**, *9*, 356 – 357.

[29] D. A. Forsyth, A. B. Sebag, *J. Am. Chem. Soc.* **1997**, *119*, 9483 – 9494.

[30] S. Shirokawa, M. Kamiyama, T. Nakamura, M. Okada, A. Nakazaki, S. Hosokawa, S. Kobayashi, *J. Am. Chem. Soc.* **2004**, *126*, 13604 – 13605.

[31] T. Nakamura, M. Harachi, T. Kano, Y. Mukaeda, S. Hosokawa, *Org. Lett.* **2013**, *15*, 3170 – 3173.

[32] L. De Luca, G. Giacomelli, S. Masala, A. Porcheddu, *J. Org. Chem.* **2003**, *68*, 4999 – 5001.

[33] a) J. Krüger, E. M. Carreira, *J. Am. Chem. Soc.* **1998**, *120*, 837 – 838; b) B. L. Pagenkopf, J. Krüger, A. Stojanovic, E. M. Carreira, *Angew. Chem. Int. Ed.* **1998**, *37*, 3124 – 3126; *Angew. Chem.* **1998**, *110*, 3312 – 3314.

[34] R. K. Boeckman, J. R. Pruitt, *J. Am. Chem. Soc.* **1989**, *111*, 8286 – 8288.

[35] a) A. Baerga-Ortiz, B. Popovic, A. P. Siskos, H. M. O'Hare, D. Spiteller, M. G. Williams, N. Campillo, J. B. Spencer, P. F. Leadlay, *Chem. Biol.* **2006**, *13*, 277 – 285; b) A. T. Keatinge-Clay, *Nat. Prod. Rep.* **2016**, *33*, 141 – 149.

[36] J. M. Winter, M. Sato, S. Sugimoto, G. Chiou, N. K. Garg, Y. Tang, K. Watanabe, *J. Am. Chem. Soc.* **2012**, *134*, 17900 – 17903.

[37] a) J. Kennedy, K. Auclair, S. G. Kendrew, C. Park, J. C. Vederas, C. R. Hutchinson, *Science* **1999**, *131*, 8388 – 8389; b) X. Xie, M. J. Meehan, W. Xu, P. C. Dorrestein, Y. Tang, *J. Am. Chem. Soc.* **2009**, *131*, 8388 – 8389.

[38] Y. Li, N. Lan, L. Xu, Q. Yu, *Appl. Microbiol. Biotechnol.* **2018**, *102*, 9881 – 9891.

[39] Y.-M. Chiang, E. Szewczyk, T. Nayak, A. D. Davidson, J. F. Snachez, H.-C. Lo, H. Wen-Yueh, H. Simityan, E. Kuo, A. Praseuth, K. Watanabe, B. R. Oakley, C. C. C. Wang, *Chem. Biol.* **2008**, *15*, 527 – 532.

[40] C. D. Reeves, Z. Hu, R. Reid, J. T. Kealey, *Appl. Environ. Microbiol.* **2008**, *74*, 5121 – 5129.

[41] R. V. K. Cochrane, Z. Gao, G. R. Lambkin, W. Xu, J. M. Winter, S. L. Marcus, Y. Tang, J. C. Vederas, *ChemBioChem* **2015**, *16*, 2479 – 2483.

[42] L. C. Axford, T. J. Simpson, C. L. Willis, *Angew. Chem. Int. Ed.* **2004**, *43*, 727 – 730; *Angew. Chem.* **2004**, *116*, 745 – 748.

[43] E.-M. Niehaus, K. Kleigrewe, P. Wiemann, L. Studt, C. M. K. Sieber, L. R. Connolly, M. Freitag, U. Güldener, B. Tudzynski, H.-U. Humpf, *Chem. Biol.* **2013**, *20*, 1055 – 1066.

[44] a) X. Guo, T. Liu, C. R. Valenzano, Z. Deng, D. E. Cane, *J. Am. Chem. Soc.* **2010**, *132*, 14694 – 14696; b) D. Gay, Y.-O. You, A. Keatinge-Clay, D. E. Cane, *Biochemistry* **2013**, *52*, 8916 – 8928.

[45] M.-C. Tang, C. R. Fischer, J. V. Chari, D. Tan, S. Suresh, A. Chu, M. Miranda, J. Smith, Z. Zhang, N. K. Garg, R. P. St. Onge, Y. Tang, *J. Am. Chem. Soc.* **2019**, *141*, 8198 – 8206.

[46] M. Ohtawa, S. Ogihara, K. Sugiyama, K. Shiomi, Y. Harigaya, T. nagamitsu, S. Omura, *J. Antibiot.* **2009**, *62*, 289 – 294.

[47] Z. Wasil, K. A. K. Pahirulzaman, C. Butts, T. J. Simpson, C. M. Lazarus, R. J. Cox, *Chem. Sci.* **2013**, *4*, 3845 – 3856.

Manuscript received: August 8, 2021
Accepted manuscript online: August 26, 2021
Version of record online: ■■ ■■, ■■■■

Research Articles

Polyketides

J. Takino, A. Kotani, T. Ozaki, W. Peng, J. Yu, Y. Guo, S. Mochizuki, K. Akimitsu, M. Hashimoto, T. Ye,* A. Minami,* H. Oikawa* _____ ■■■■–■■■■

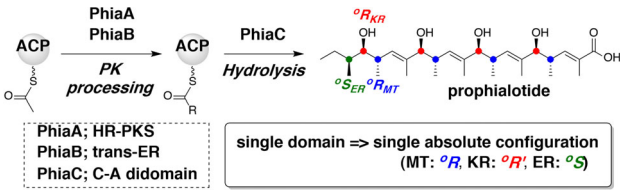

Biochemistry-Guided Prediction of the Absolute Configuration of Fungal Reduced Polyketides

We performed a focused analysis of functionally related polyketide synthases (PKSs) which produce linear polyketides (PKs) such as prophialotide and other polyhydroxy PKs. The relative and absolute configurations were determined by degradation studies. Based on the results, we propose a stereochemical rule during the chain-elongation process of the reduced PKs.